Article

Advancing the PROSPECT-5 Model to Simulate the Spectral Reflectance of Copper-Stressed Leaves

Chengye Zhang [1,2,3,4] (iD), Huazhong Ren [1,2,3] (iD), Yanzhen Liang [5], Suhong Liu [6], Qiming Qin [1,2,3,*] and Okan K. Ersoy [4]

[1] Institute of Remote Sensing and Geographic Information System, School of Earth and Space Sciences, Peking University, Beijing 100871, China; zhangchengye@pku.edu.cn (C.Z.); renhuazhong@pku.edu.cn (H.R.)

[2] Beijing Key Lab of Spatial Information Integration and 3S Application, Peking University, Beijing 100871, China

[3] Mapping and Geo-Information for Geographic Information Basic Softwares and Applications, Engineering Research Center of National Administration of Surveying, Beijing 100871, China

[4] School of Electrical and Computer Engineering, Purdue University, West Lafayette, IN 47907, USA; ersoy@purdue.edu

[5] Earth Observation System & Data Center, China National Space Administration, Beijing 100101, China; xueer3329@163.com

[6] Faculty of Geographical Science, Beijing Normal University, Beijing 100875, China; liush@bnu.edu.cn

* Correspondence: qmqinpku@163.com; Tel.: +86-10-6276-5715

Abstract: This paper proposes a modified model based on the PROSPECT-5 model to simulate the spectral reflectance of copper-stressed leaves. Compared with PROSPECT-5, the modified model adds the copper content of leaves as one of input variables, and the specific absorption coefficient related to copper (K_{cu}) was estimated and fixed in the modified model. The specific absorption coefficients of other biochemical components (chlorophyll, carotenoid, water, dry matter) were the same as those in PROSPECT-5. Firstly, based on PROSPECT-5, we estimated the leaf structure parameters (N), using biochemical contents (chlorophyll, carotenoid, water, and dry matter) and the spectra of all the copper-stressed leaves (samples). Secondly, the specific absorption coefficient related to copper (K_{cu}) was estimated by fitting the simulated spectra to the measured spectra using 22 samples. Thirdly, other samples were used to verify the effectiveness of the modified model. The spectra with the new model are closer to the measured spectra when compared to that with PROSPECT-5. Moreover, for all the datasets used for validation and calibration, the root mean square errors (RMSEs) from the new model are less than that from PROSPECT-5. The differences between simulated reflectance and measured reflectance at key wavelengths with the new model are nearer to zero than those with the PROSPECT-5 model. This study demonstrated that the modified model could get more accurate spectral reflectance from copper-stressed leaves when compared with PROSPECT-5, and would provide theoretical support for monitoring the vegetation stressed by copper using remote sensing.

Keywords: vegetation remote sensing; reflectance model; spectra; leaf; copper; PROSPECT

1. Introduction

Remote sensing provides a rapid and large-scale tool for geobotanical prospecting [1–3] and environmental monitoring [4]. For the vegetation on copper deposits or the area polluted by industrial activities related to copper, excessive copper elements would be absorbed by root systems, and then stress the growth of plants and change the spectral reflectance of leaves. In addition, spectral reflectance is the vital foundation of vegetation remote sensing. Hence, the reflectance of leaves on copper-stressed

vegetation is crucial for prospecting copper deposit and monitoring copper-pollution. Currently, most studies on remote sensing of vegetation stressed by heavy metal or other stress factors focus on the change of reflectance and vegetation indices using empirical statistical methods; many statistical models have been proposed, but little research has focused on the physical model [4–10]. However, for many users, statistical models cannot meet the requirement for understanding the action mechanism of copper (Cu) stress on leaf reflectance. Moreover, many parameters in statistical models are sensitive to the case study and have no physical meaning. Hence, a model that can accurately simulate the spectral reflectance of copper-stressed leaves should be developed, which would compensate for some of the deficiencies of statistical models.

The PROSPECT leaf optical properties model has been an important and most popular physical model to simulate leaf directional hemispherical reflectance and transmittance from 400 to 2500 nm [11,12]. Here we review the evolution over time of PROSPECT in order to illustrate the novelty of our study. To explain the interaction of isotropic light with a compact leaf, a theoretical model called "Plate Model" was proposed, which regards a compact leaf as an absorbing plate [13]. Plate Model was later generalized to the non-compact leaf [14]. Based on the generalized Plate Model, the PROSPECT model was proposed to simulate the spectral reflectance and transmittance of a leaf [11]. In this initial version, the reflectance and transmittance were calculated by the refractive index (n), a parameter describing the leaf structure (N), pigment concentration (C_{ab}), equivalent water thickness (C_w), and the corresponding specific absorption coefficients (K_{ab} and K_w), where n, K_{ab} and K_w, have been fitted by data with varying plant types and status. After this version, the content (C_m) and corresponding specific absorption coefficient (K_m) of the dry matter that influences the absorption features in shortwave infrared (SWIR), including cellulose, lignin, protein, hemicellulose, starch, and sugar, were introduced into the PROSPECT model [15–19]. The spectral resolution was improved from 5 nm to 1 nm in an unreleased version [20,21], and the model was modified to account for surface directional reflectance of a leaf [21,22]. In 2008, the PROSPECT model was further calibrated and two new versions (PROSPECT-4 and PROSPECT-5) were proposed [21]. The difference between PROSPECT-4 and PROSPECT-5 is that PROSPECT-5 separates total carotenoids from total pigments. In recent years, PROSPECT-5 has been popularly used in the remote sensing of vegetation instead of other versions.

However, the PROSPECT versions above were developed for healthy leaves. For copper-stressed leaves, excessive copper would change the spectral reflectance of leaves. Hence, to simulate the reflectance of copper-stressed leaves, the copper content and the specific absorption coefficient related to copper was added into the PROSPECT model [23]. Zhu et al. [23] initiated research on the physical reflectance model of copper-stressed leaves. However, in [23], there are still some problems needing to be addressed, whereas subsequent studies were not found in public literatures. These problems are shown as follows. (1) The structure parameter N of copper-treated leaf is determined using the reflectance at 800–1200 nm, and the absorption of copper ion was ignored in this wavelength range in the [23]. However, according to the theory of electron transition and experimental observation [24], there is a significant absorption of copper ion at 700–900 nm. (2) Carotenoid content has been treated as an input variable in the popular PROSPECT-5 model and has important influence on the reflectance of leaves. However, the carotenoid content and its specific absorption coefficient were ignored in the model developed in [23]. (3) The absorption characteristics of biochemical components (water, chlorophyll, dry matter, pigment) are inherent and should be remained unchanged in the advanced model for copper-stressed leaves.

Hence, based on above problems, the study on the reflectance model of copper-stressed leaves should be continued. In other words, the specific absorption coefficient related to copper needs to be improved, and a more accurate model for simulating the reflectance of copper-stressed leaf should be developed. Based on this motivation, we estimated the specific absorption coefficient related to copper and added it into the popular PROSPECT-5 model, and then developed a modified model to simulate the reflectance of copper-stressed leaf. The proposed model considers the carotenoid content,

copper content and corresponding specific absorption coefficients. In addition, it avoids the coupling influence on the reflectance from structure parameter N and the absorption of copper ions.

2. Datasets

In this study, wheat (*Triticum aestivum* L., cultivar: "Xinchun-17") and pak choi (*Brassica chinensis* L., cultivar: "Shanghaiqing") were treated by copper with different levels using control experiments. Soil was collected from a vegetable garden without any contamination. Seeds were planted in the soil mixed with copper sulfate ($CuSO_4$) solutions in impermeable plastic pots (Figure 1). The copper contents in soil were controlled as 0, 25, 50, 100, 200, 400, 800, 1600, 3200, and 4800 mg/kg, respectively. The pot distribution of wheat and experimental scene of some samples are shown in Figure 1, and the pot distribution of pak choi is same as that of wheat. Therefore, the total number of pots is 60. For the group with 0 mg/kg copper content, the plants were regarded as healthy vegetation. Thus, the data from this group was not used for the calibration of the reflectance model for copper-stressed vegetation. This group was only used as a reference for observing the growth of copper-stressed vegetation. There are same characteristics (except copper content) of the experimental soil with different Cu levels, including nitrogen (N) content, phosphorus (P) content, potassium (K) content, water content, particle size, pH, and so forth. There are three pots for each copper-stress level experiment (three parallel experiments) to reduce accidental errors (Figure 1).
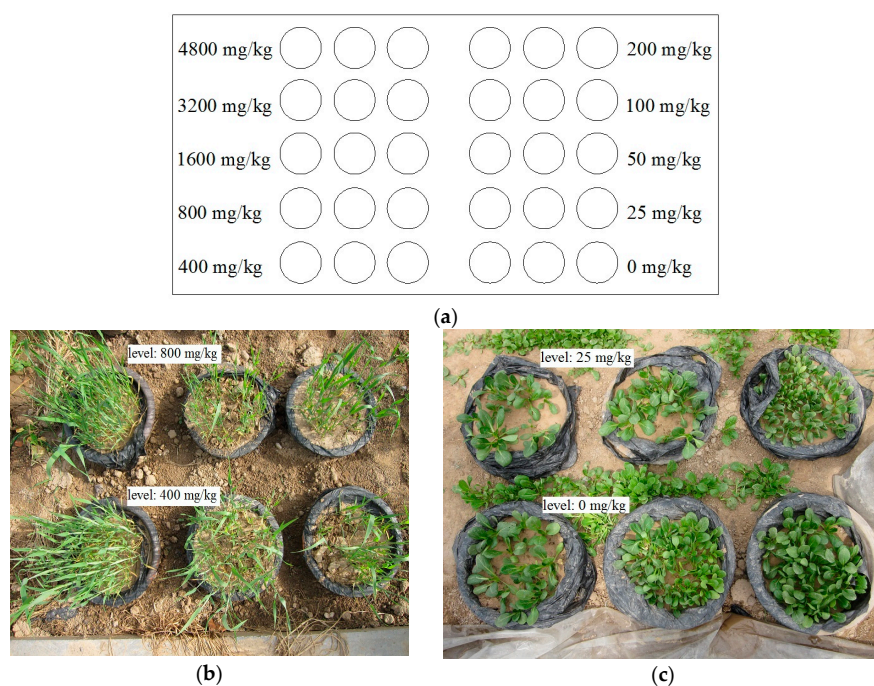

Figure 1. The experimental scene of some samples: (**a**) The distribution of plastic pots of wheat. (The pots distribution of pak choi is same with that of wheat. Circle: a pot); (**b**) Some samples of wheat (stress level: 400 mg/kg; 800 mg/kg); (**c**) Some samples of pak choi (stress level: 0 mg/kg; 25 mg/kg).

The spectral reflectance of leaves was measured by ASD (Analytical Spectral Devices) FieldSpec FR spectroradiometer (Boulder, CO, USA) with an Li-1800 integrating sphere (Li-Cor, Lincoln, NE, USA). The inside of the sphere is covered with $BaSO_4$. The diameter of sample port of the integrating sphere is about 14 mm, which could be covered by the measured leaves. The standard white reference was measured (the fiber faced the sample port) before each measurement of a sample (the fiber faced the reference). The light source is a halogen lamp. Due to the data quality from 1650 to 2500 nm from the integrating sphere, auxiliary spectra were also measured with a leaf clip, and these spectra from 1650 to 2500 nm were linearly scaled to replace the corresponding data from the integrating sphere.

In future studies, other integrating spheres with better data (e.g., RT-060-SF, Labsphere, NH, USA) are recommended to readers. The wavelength range of final measured spectra was from 350 to 2500 nm, and the spectral resolution was 1 nm, which is the same as that of the PROSPECT-5 model.

After the reflectance measurement in the laboratory, the leaves were immediately processed to measure biochemical components. Thus, the changing of biochemical components with different hours in a day almost has no impact in this study. The content (per surface area unit) of every biochemical component (i.e., chlorophyll, carotenoid, water, dry matter, and copper) in the leaves was measured using corresponding chemical methods. In detail, for each measurement, the leaf was sampled using a puncher with a hole of a known area. For the chlorophyll and carotenoid of a sample, the sample was triturated and then 80% acetone was used for extracting the chlorophyll and carotenoid. The absorbance of the solution was measured by a spectrophotometer at 470 nm, 646 nm, and 663 nm [23,25]. The concentration (mg/L) of chlorophyll and carotenoid was calculated based on the quantitative relationship between absorbance and pigment concentration (Lambert-Beer Law) [23,25]. According to the volume of the solution and the surface area of sample, the content (per surface area unit) of chlorophyll and carotenoid in a sample can be determined. For the measurement of copper content, the leaf sample was digested in concentrated nitric acid and perchloric acid. The solution was filtered, and the copper concentration was determined by atomic absorption spectrophotometry [23,26]. For the measurement of water content and dry matter content, the leaves were continuously heated at 105 °C for 30 min to kill the leaves to cease the metabolism and avoid some matter decomposition in the next step. The leaves were dried at 70 °C to get a constant weight, and then the leaves were weighed to determine the content of water and dry matter. Hence, for each sample, data on the content (per surface area unit) of copper, chlorophyll, carotenoid, water, and dry matter were collected as well as the corresponding spectral reflectance.

In addition, the images of internal structure of leaves with different stress levels were acquired by scanning electron microscopy (SEM). The samples were processed by freeze fracture technique and immediately put into the 2% glutaraldehyde solution (solvent: 0.1 mol/L potassium phosphate buffer, pH = 7.2). All the samples were preserved at constant 4 °C and observed with SEM [23]. The SEM used in this study was KYKY-EM 3200 with a resolution better than 6 nm.

In this study, the leaves were collected at different growth stages of the two vegetation (wheat: elongation stage, heading stage; pak choi: six leaves period, eight leaves period). The leaves sampled were the visually representative leaves in the plant. With the exception of the normal leaves (stress level = 0 mg/kg) and outliers, 33 groups of datasets of copper-stressed leaves were finally used for this study. The 33 groups of datasets of copper-stressed leaves were randomly divided into two parts (22 groups and 11 groups). Twenty-two groups of datasets were used to develop the new model, and the remaining 11 groups were used to perform validation of the new model.

In addition, this study also used a public dataset named LOPEX93 [27] for the comparison with the data of copper-stressed leaves on the leaf structure parameters. The LOPEX93 dataset includes the biochemical components and spectra of a variety of plants and has been widely used in the remote sensing of vegetation. In this study, the LOPEX93 dataset was downloaded from the website in [28].

3. Methods

In the PROSPECT model, a leaf is assumed to be composed of N homogeneous compact layers of biochemical components separated by $(N - 1)$ layers of air. N described the overall characteristics of the leaf structure and varies with different leaves. In the PROSPECT-5 version, the following parameters have been estimated and fixed in the model, and these parameters do not vary with different leaves: the angle of incidence of incoming radiation (α), refractive index ($n(\lambda)$), specific absorption coefficient of each biochemical components ($K_{ab}(\lambda)$, $K_{car}(\lambda)$, $K_w(\lambda)$, and $K_m(\lambda)$ represent the specific absorption coefficient of chlorophyll, carotenoid, water, and dry matter, respectively); $n(\lambda)$, $K_{ab}(\lambda)$, $K_{car}(\lambda)$, $K_w(\lambda)$, and $K_m(\lambda)$ are the functions of wavelength λ. Since above parameters were fixed,

the simulations for the spectral reflectance of different leaves depend on the absorption coefficient of a compact layer ($K(\lambda)$).

The calculation method of $K(\lambda)$ is given by Equation (1) in PROSPECT-5 [21].

$$K(\lambda) = \frac{K_{ab}(\lambda) \cdot C_{ab} + K_{car}(\lambda) \cdot C_{car} + K_w(\lambda) \cdot C_w + K_m(\lambda) \cdot C_m}{N}, \qquad (1)$$

where C_{ab}, C_{car}, C_w, C_m are the contents of chlorophyll, carotenoid, water (equivalent water thickness), and dry matter in leaf, respectively. Hence, to simulate the spectral reflectance of different leaves, following parameters which varies with different leaves are the five input variables of PROSPECT-5: N, C_{ab}, C_{car}, C_w, C_m. In other words, the PROSPECT-5 considers the absorption of four biochemical components: chlorophyll; carotenoid; water, and; dry matter.

However, several studies have indicated that heavy metal stress would damage the leaf structure, leading to a disorderly cell arrangement (e.g., [23,29]). Moreover, the copper content in copper-stressed leaf could be approximately 100 times more than that in normal leaf, so the absorption related to copper should not be ignored in the new model. Hence, we further analyzed the leaf structure parameter (N) and the specific absorption coefficient related to copper. Thus, α, $n(\lambda)$, $K_{ab}(\lambda)$, $K_{car}(\lambda)$, $K_w(\lambda)$, and $K_m(\lambda)$, which were analyzed and determined in PROSPECT-5 [21], were used in the new model with no change, because there are no existing studies or theories that link these parameters to copper stress.

The flowchart of the method used in this study is shown in Figure 2. (1) The leaf structure parameters of all the 33 samples were estimated by fitting the simulated spectra to the measured spectra in 400–510 nm using PROSPECT-5. The detailed method for calculating N could be found in Section 3.1; (2) 22 samples were used to estimate the specific absorption coefficient related to copper. The leaf structure parameter N and the specific absorption coefficient related to copper were determined independently in this study; (3) Other samples were used for the validation of the modified model. This procedure is explained in detail in Sections 3.1–3.3.

The modified model considers the absorption related to copper and adds the content of copper (C_{cu}) as an input variable when compared with PROSPECT-5. The input variables of both the modified model and the PROSPECT-5 model could be read from Table 1. In fact, only the content of copper (C_{cu}) was added to the modified model when it is compared with PROSPECT-5 (Table 1).
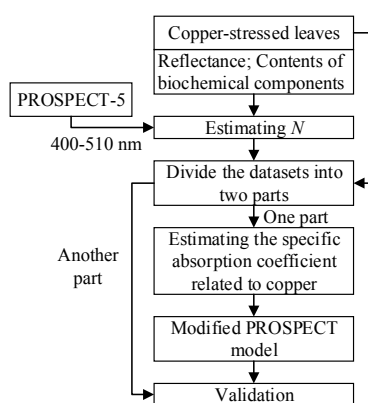

Figure 2. The steps of the method used in this study.

Table 1. The input variables of the modified model and the PROSPECT-5 model (for comparison).

Model	PROSPECT-5	Modified Model
Leaf structure parameter	N	N
Content of chlorophyll	C_{ab}	C_{ab}
Content of carotenoid	C_{car}	C_{car}
Equivalent water thickness	C_w	C_w
Content of dry matter	C_m	C_m
Content of copper	/	C_{cu}

3.1. Determination of N under Copper Stress

As previously mentioned, excessive copper in a plant would damage the leaf structure, which would result in a disorderly cell arrangement ([23,29]). To further illustrate the change of internal structure of copper-stressed leaves, some SEM images of leaves with different levels of copper stress are shown in Figure 3. It is clearly observed that more disordered internal structure was present in higher-stressed leaves, including atrophic mesophyll cells, disintegrating vascular bundle, and disorderly cell arrangement.

The PROSPECT model regards the leaf as N homogeneous compact layers of plates separated by $(N-1)$ layers of air. The leaf structure parameter (N) describes the leaf mesophyll structure and increases with a more disorderly cell arrangement. The value of N should be estimated accurately when the PROSPECT model is used for simulating the spectral reflectance of leaf.

The influence from the absorption by regular biochemical components at 800–1300 nm is the minimum in the whole wavelength. Moreover, the specific absorption coefficients of regular biochemical components is unknown and also needed to be estimated in the previous calibration on PROSPECT for healthy leaves ([21,23]). Hence, in previous studies on PROSPECT, the range of 800–1300 nm was selected for estimating N to avoid the influence from the absorption by regular biochemical components ([21,23]).

However, in this study, the specific absorption coefficients of above biochemical components in PROSPECT-5 remained unchanged in the modified model and did not need to be recalculated. So the influence from the absorption by regular biochemical components did not need to be considered. For estimating N in this study, the real influence may come from the absorption related to copper and the specific absorption coefficient related to copper was not yet determined. Hence, a wavelength range where the absorption of copper is at minimum should be selected to determine N of copper-stressed leaves to avoid the coupling influence. The absorption spectra of aqueous copper sulfate solutions were measured in [24], and the results demonstrated that the absorption of copper sulfate solutions almost equals zero in the range from 400 to 510 nm. As the wavelength λ ranges from 400 to 2500 nm in Equation (1), the reflectance in the whole wavelength would vary with different N. To verify this point and observe the detailed influence from N on the reflectance at 400–510 nm, the contents of biochemical components were fixed, and a series of reflectance spectra were generated with varying N. Figure 4 shows that changing N would cause the changes of reflectance in the whole wavelength range (400 to 2500 nm), including 400–510 nm. Therefore, we selected 400–510 nm, not 800–1300 nm, to estimate N.

In this study, we estimated the N of j-th leaf (N_j) by minimizing the merit function given by Equation (2) from 400 to 510 nm. In detail, for a leaf, the method is to find the minimum $J(N_j)$ and the corresponding N when N ranges from 1 to 7 with step = 0.01.

$$J(N_j) = (R_{mes,j}(\lambda_1) - R_{sim,j}(N_j, \lambda_1))^2 + (R_{mes,j}(\lambda_2) - R_{sim,j}(N, \lambda_2))^2, \tag{2}$$

where $R_{mes,j}$ and $R_{sim,j}$ are the j-th measured reflectance and corresponding modeled reflectance at the wavelength λ_1 and λ_2, respectively. The wavelengths λ_1 and λ_2 were where the measured reflectance reached maximum and minimum, respectively.

The leaf structure parameter N varies with different leaves and is a necessary input variable for both PROSPECT-5 and the modified model (Table 1). In this study, the leaf structure parameters N of 22 samples need to be estimated and then need to be used in the PROSPECT-5 model to calculate the specific absorption coefficient related to copper. The leaf structure parameters N of 11 samples for validation also need to be estimated to simulate the spectral reflectance of copper-stressed leaves using the modified model. Hence, the leaf structure parameters of all the samples need to be estimated. According to Equation (2), the calculation for N in a sample is independent and has nothing to do with other samples. Therefore, in this study, the leaf structure parameters N were estimated sample by sample, and the N of all the 33 copper-stressed samples were estimated.
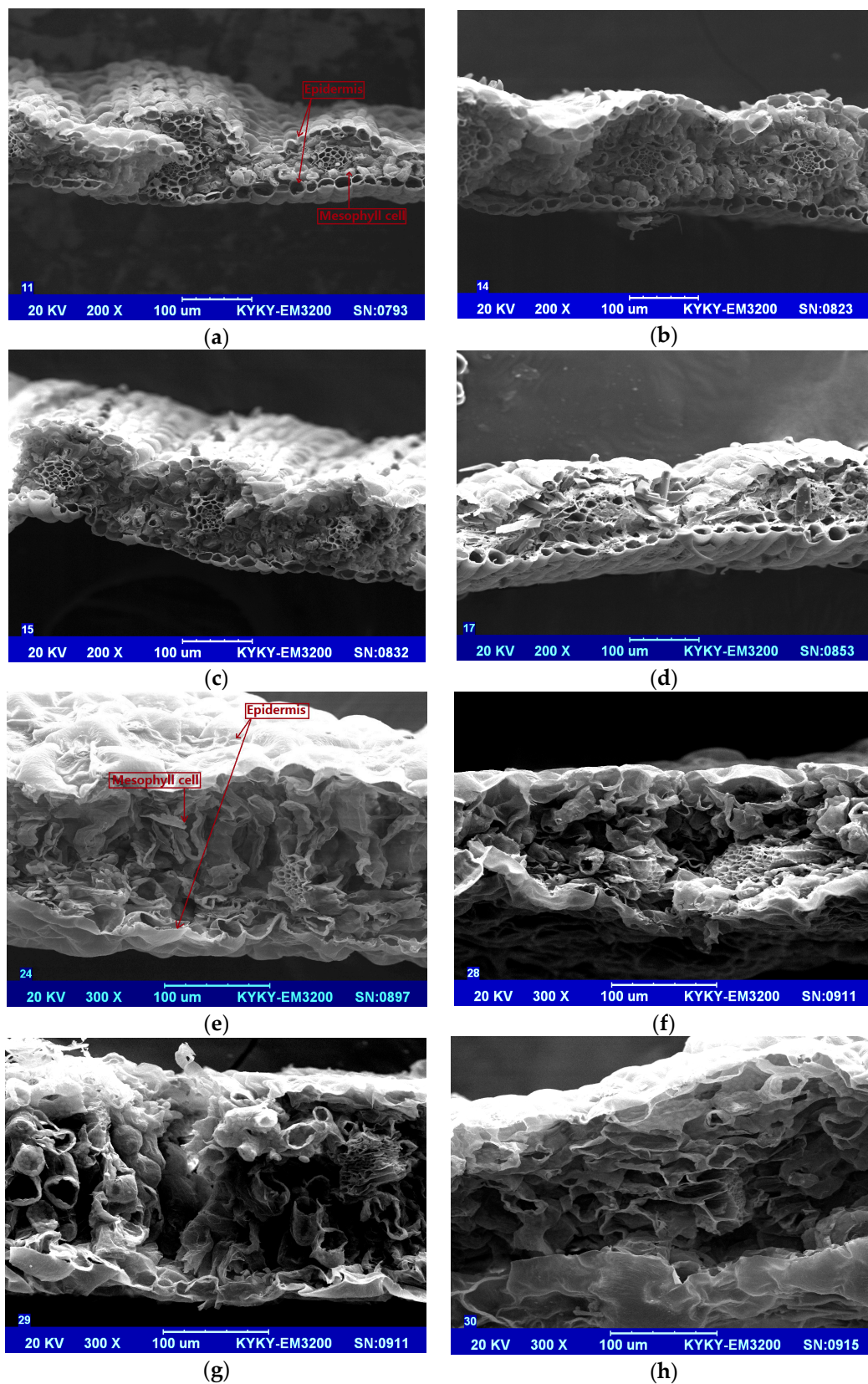
Figure 3. Scanning electron microscopy (SEM). images of leaves with different copper contents in soil: (**a**) Normal wheat; (**b**) Wheat with 200 mg/kg copper content in soil; (**c**) Wheat with 400 mg/kg copper content in soil; (**d**) Wheat with 1600 mg/kg copper content in soil; (**e**) Normal pak choi; (**f**) Pak choi with 200 mg/kg copper content in soil; (**g**) Pak choi with 400 mg/kg copper content in soil; (**h**) Pak choi with 800 mg/kg copper content in soil.
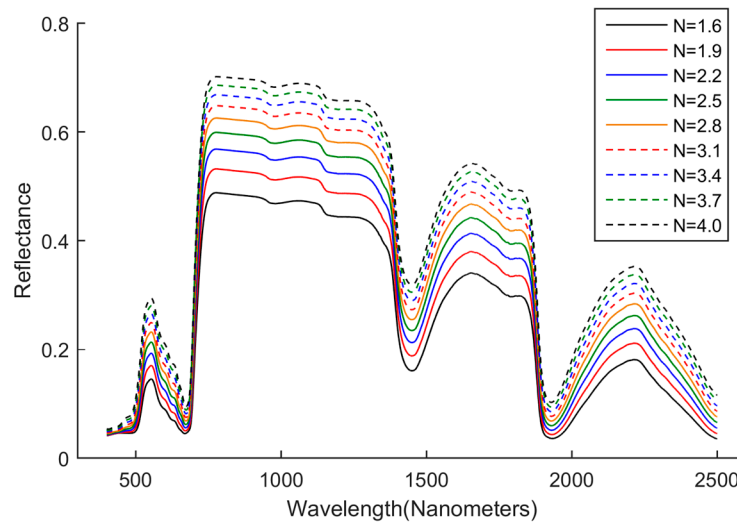
Figure 4. The modeled reflectance generated by PROSPECT-5 with different *N*. (C_{ab}, C_{car}, C_w, and C_m are fixed as 33 μg/cm^2, 8.6 μg/cm^2, 0.012 cm, 0.005 g/cm^2, respectively).

3.2. Determination of Specific Absorption Coefficient Related to Copper

Copper content in a healthy leaf is normally 5 to 30 mg/kg [4]. However, as previously mentioned, the copper content in a copper-stressed leaf would be approximately 100 times more than that in a normal leaf, which has been verified by the measured results from several previous studies (e.g., [4,6]). Hence, the absorption related to copper should be considered, and thus the calculation method of $K(\lambda)$ was modified as Equation (3).

$$K_{new}(\lambda) = \frac{K_{ab}(\lambda) \cdot C_{ab} + K_{car}(\lambda) \cdot C_{car} + K_w(\lambda) \cdot C_w + K_m(\lambda) \cdot C_m + K_{cu}(\lambda) \cdot C_{cu}}{N}, \tag{3}$$

where K_{cu} and C_{cu} are the specific absorption coefficient related to copper and the copper content in leaf, respectively. $K_{new}(\lambda)$ is the absorption coefficient in the new model.

The estimating method of K_{cu} in this study was similar with the methods for estimating specific absorption coefficients of other biochemical components in [21,23]. At each wavelength, we minimized the merit function given by Equation (4).

$$J(K_{cu}(\lambda)) = \sum_{j=1}^{Num} (R_{mes,j}(\lambda) - R_{sim,j}(K_{new}(\lambda), \lambda))^2, \tag{4}$$

where $R_{mes,j}(\lambda)$ and $R_{sim,j}(K_{cu}(\lambda), \lambda)$ are the *j*-th measured reflectance and corresponding modeled reflectance at the wavelength λ. *Num* is the number of samples for estimating K_{cu}. In this study, *Num* = 22.

An illustration on the modification strategy in this study should be presented here. The reflectance from 400 to 510 nm is controlled mainly by chlorophyll and carotenoids. Copper almost has no direct contribution to the reflectance from 400 to 510 nm. Although the copper-induced physiological implications (change of pigments) could affect the reflectance from 400 to 510 nm, this effectiveness should not be considered when the two pigments were measured correctly. Hence, the leaf structure parameter *N* was determined in the wavelengths from 400 to 510 nm since parameters of chlorophyll and carotenoids are known. In addition, the leaf structure parameter *N* and K_{cu} can be determined independently since *N* can be estimated by using reflectance spectra over the spectral range with no copper-related absorption.

3.3. Validation of the Modified Model

In this study, 11 groups of datasets on copper-stressed leaves were used for the validation of the new model. The simulated reflectance spectra were generated using PROSPECT-5 and the new model with the estimated *N*, respectively. The mean (±standard deviation, SD) of the simulated spectra and measured spectra of the 11 samples were calculated for comparison. The simulated spectra and measured spectra of two selected representative samples (No. 5 and No. 7) from 11 samples were also used for comparison. By observing the spectra, the modified model will be better than PROSPECT-5 if the spectra with the modified model is closer to the measured spectra. The differences between simulated reflectance and measured reflectance at seven key wavelengths, including 550 nm, 660 nm, 700 nm, 850 nm, 1400 nm, 1900 nm, and 2200 nm, were calculated. The modified model will be better than PROSPECT-5 if the differences with the modified model are nearer to zero than those with the PROSPECT-5 model. The root mean square error (RMSE) between the simulated spectra and measured spectra were calculated for both calibration and validation samples. The modified model will be better than PROSPECT-5 if the RMSEs with the modified model are less.

4. Results

The mean, standard deviation (SD), and coefficient of variation (CV) of datasets for calibration and validation were calculated (Table 2). Coefficient of variation characterizes the inter-difference degree in a dataset. In this study, all the coefficient of variations are significant high and the CVs with copper are the highest. Table 2 demonstrates that there are significant differences in leaf Cu and in other biochemical components for both calibration and validation datasets.

Table 2. Mean, standard deviation (SD), and coefficient of variation (CV) of datasets for calibration and validation (water: cm; dry matter: g/cm^2; chlorophyll, carotenoids, and copper: $\mu g/cm^2$).

	Calibration Datasets			Validation Datasets		
	Mean	**SD**	**CV**	**Mean**	**SD**	**CV**
water	0.0175	0.00771	44.04%	0.0213	0.00964	45.26%
dry matter	0.0041	0.00084	20.34%	0.0042	0.00094	22.08%
chlorophyll	32.64	7.853	24.06%	33.79	8.062	23.86%
carotenoids	13.36	5.942	44.48%	15.67	7.388	47.15%
copper	0.1220	0.09784	80.22%	0.1507	0.1571	104.22%

In this study, the leaf structure parameters *N* were estimated sample by sample, and the results of estimating *N* of all the 33 copper-stressed samples are presented here (Figure 5a). In addition, we randomly selected 33 groups of leaf structure parameters of normal leaves from the LOPEX93 dataset [27], which is also shown in Figure 5a. The box-and-whisker plots of the *N* of copper-stressed leaves and normal leaves are shown in Figure 5b. Figure 5a,b show that the leaf structure parameters of copper-stressed leaves are obviously more than those of normal leaves. Moreover, the distributed range of *N* with copper-stressed leaves is larger. The leaf structure parameters vs. leaf copper content with different symbols for each species were plotted in Figure 5c. The stress datasets were divided into three parts based on stress levels (low, medium, high). The averages of leaf structure parameters were plotted in Figure 5d for different classes and species. Figure 5c,d show that the leaf structure parameters tend to increase with stress levels.

The estimated specific absorption coefficient related to copper (K_{cu}) is shown in Figure 6. Following characteristics could be read from Figure 6: K_{cu} is near zero from 400 to 510 nm. High values of K_{cu} are presented at 590–710 nm with a valley near 680 nm, respectively. In addition, there are three major peaks near 1400 nm, 1900 nm, and 2400 nm, respectively.
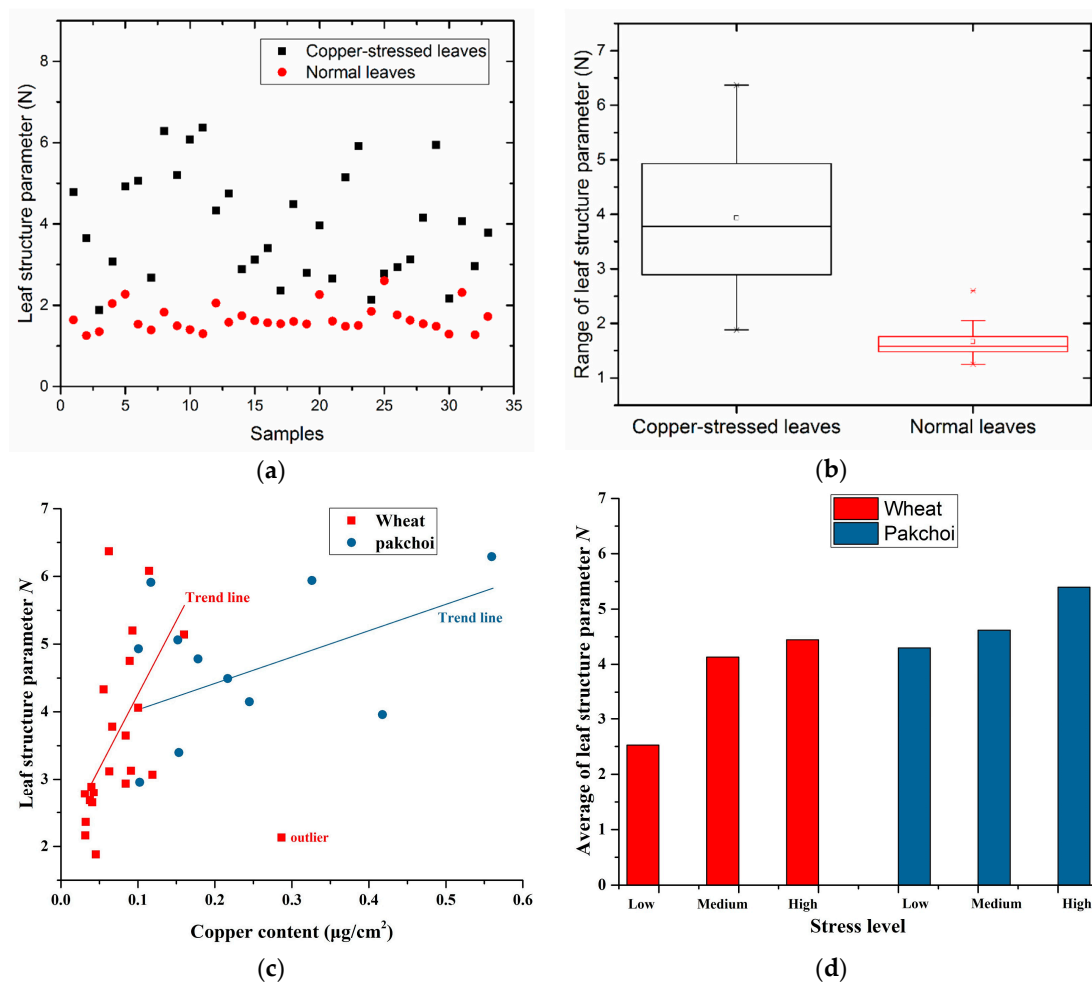
Figure 5. Leaf structure parameters *N* of copper-stressed leaves and normal leaves: (**a**) The value of leaf structure parameters; (**b**) The box-and-whisker plots of leaf structure parameters; (**c**) Leaf structure parameters vs. leaf copper content with different symbols for each species; (**d**) Bar graphs for the average of different stress levels (low, medium, high) and species.
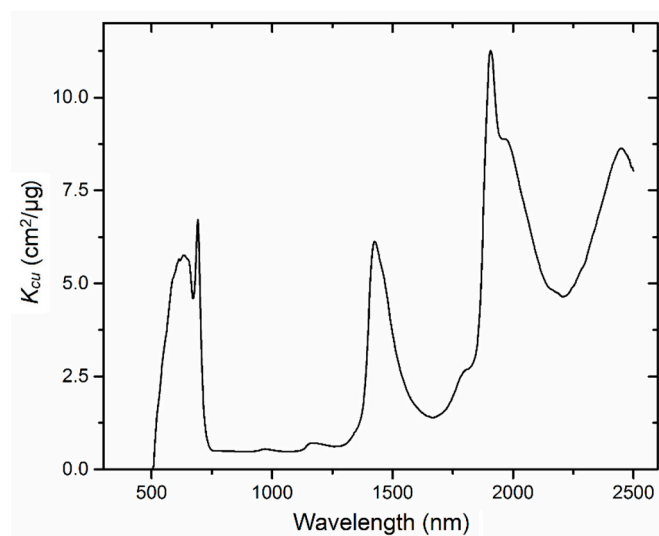

Figure 6. The specific absorption coefficient related to copper (K_{cu}).

The mean (±standard deviation, SD) of simulated spectra and measured spectra of the 11 samples is shown in Figure 7a. The simulated spectra and measured spectra of two selected representative samples (No. 5 and No. 7) from 11 samples are shown in Figure 7b,c. Samples of No. 5 and No. 7 are from wheat and pak choi, respectively. Figure 7 shows that, in the whole range of wavelength, the values of spectral reflectance with PROSPECT-5 are larger than the measured values, while the spectral reflectance with the new model is closer to the measured spectra. The 11 groups of RMSEs between the simulated spectra (PROSPECT-5 and the new model) and measured spectra are shown in Table 3. We also calculated the RMSE of each model for the calibration datasets (Table 4). For all the datasets used for validation and calibration, the RMSEs from the new model are less than that from PROSPECT-5.
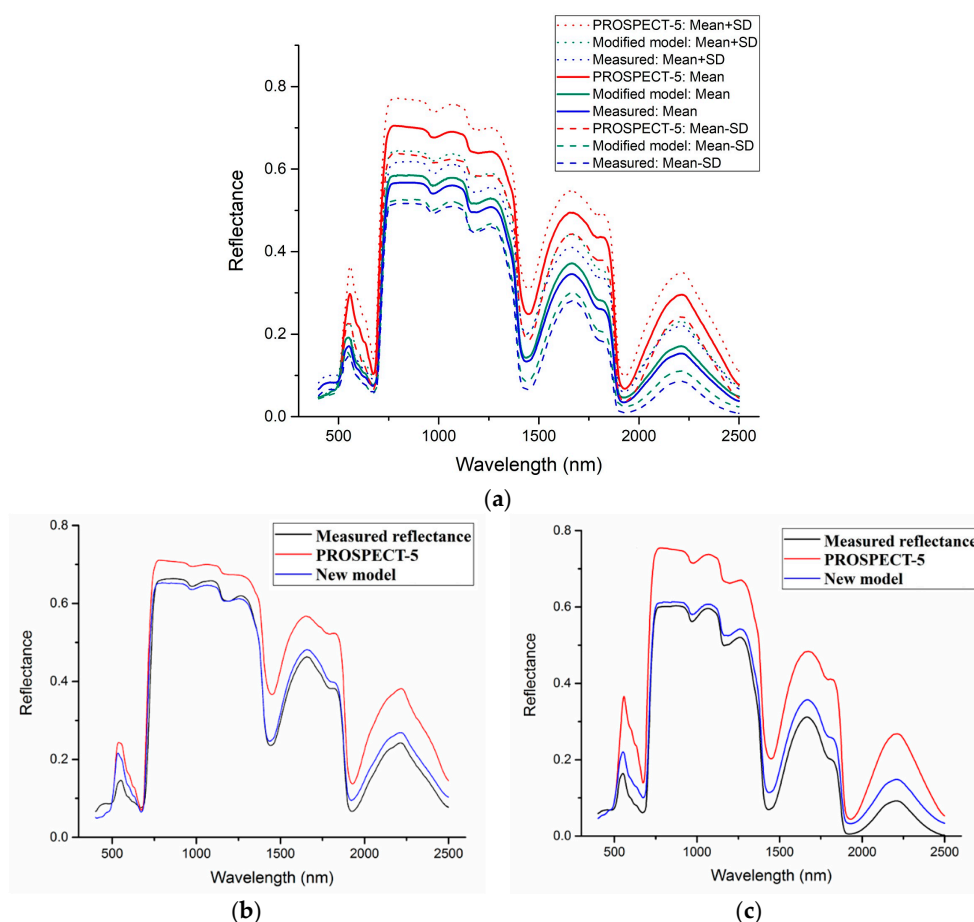

Figure 7. The simulated spectra (PROSPECT-5 and the new model) and measured spectra: (**a**) The mean (±standard deviation, SD) of simulated spectra and measured spectra of the 11 samples; (**b**) The selected representative sample: No. 5 sample (wheat: C_{ab} = 49.63 µg/cm^2; C_{car} = 8.94 µg/cm^2; C_w = 0.0096 cm; C_m = 0.0061 g/cm^2; C_{cu} = 0.0557 µg/cm^2); (**c**) The selected representative sample: No. 7 sample (pak choi: C_{ab} = 27.61 µg/cm^2; C_{car} = 19.32 µg/cm^2; C_w = 0.0320 cm; C_m = 0.0031 g/cm^2; C_{cu} = 0.1520 µg/cm^2).

To further illustrate the effectiveness of the new model, the reflectance values at several key wavelengths were selected for comparison where the reflectance curve of vegetation shows peaks, valleys, or obvious high values, including 550 nm, 660 nm, 700 nm, 850 nm, 1400 nm, 1900 nm, and 2200 nm. We calculated the differences between simulated reflectance and measured reflectance at these seven key wavelengths, and plotted these differences vs. wavelength and 11 samples, including

wheat and pak choi (samples 1–6: wheat; samples 7–11: pak choi) (Figure 8). Figure 8 shows that the differences with the modified model are nearer to zero than those with the PROSPECT-5 model.
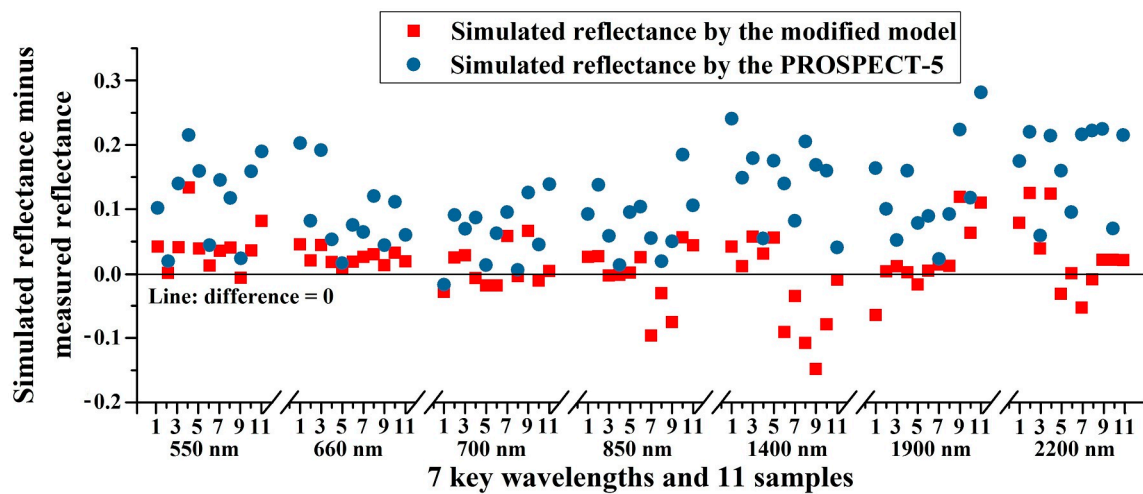

Figure 8. Differences between simulated reflectance and measured reflectance at key wavelengths.

Table 3. Root mean square errors (RMSEs) between the simulated spectra (PROSPECT-5 and the new model) and measured spectra of 11 groups samples used for validation.

Samples	No. 1	No. 2	No. 3	No. 4	No. 5	No. 6
PROSPECT-5	0.1567	0.1685	0.0810	0.0613	0.0988	0.0708
New model	0.0776	0.0576	0.0261	0.0225	0.0265	0.0486
Samples	**No. 7**	**No. 8**	**No. 9**	**No. 10**	**No. 11**	
PROSPECT-5	0.1489	0.1492	0.0781	0.1874	0.1924	
New model	0.0395	0.0942	0.0135	0.1038	0.0190	

Table 4. RMSEs between the simulated spectra (PROSPECT-5 and the new model) and measured spectra of 22 groups of samples used for calibration.

Samples	No. 1	No. 2	No. 3	No. 4	No. 5	No. 6
PROSPECT-5	0.1619	0.1943	0.1741	0.1444	0.1437	0.1489
New model	0.0943	0.1261	0.0496	0.0563	0.0491	0.0488
Samples	**No. 7**	**No. 8**	**No. 9**	**No. 10**	**No. 11**	**No. 12**
PROSPECT-5	0.1010	0.0433	0.0188	0.0791	0.0702	0.0377
New model	0.0312	0.0316	0.0173	0.0302	0.0210	0.0165
Samples	**No. 13**	**No. 14**	**No. 15**	**No. 16**	**No. 17**	**No. 18**
PROSPECT-5	0.0483	0.0543	0.1504	0.0254	0.1935	0.1214
New model	0.0175	0.0274	0.1043	0.0182	0.0949	0.0481
Samples	**No. 19**	**No. 20**	**No. 21**	**No. 22**		
PROSPECT-5	0.1328	01321	0.1347	0.1352		
New model	0.0438	0.0253	0.0112	0.0782		

5. Discussion

This paper advances the PROSPECT-5 model to simulate the reflectance of copper-stressed leaves and get accepted results of validation. There are some results needing further explanation and discussion.

The leaf structure parameters of copper-stressed leaves were estimated in the range from 400 to 510 nm, not from 800 to 1300 nm. Due to the low absorption of copper ion in this range, the estimation of the leaf structure parameters in this study avoided the influence from copper. The results of leaf structure parameters of copper-stressed leaves show three characteristics (Figure 5): they are generally larger than those of normal leaves; the distributed range is also larger; the leaf structure parameters tend to increase with stress levels. The most probable reason is that the structures of copper-stressed leaves were damaged due to excessive copper, and the cells were more disorderly with a higher level copper stress. This reason was also partially demonstrated by the SEM images (Figure 3). In addition, for estimating N in this study, we assumed the influence may come from the absorption related to copper, so we used a wavelength range where the absorption of copper ion is near zero, yet it might be that copper has other influences that we do not know about. Due to the indirect influence on reflectance from copper stress by changing the leaf structure, it is a good idea to establish a statistical relationship between N and copper content of a particular vegetation in the future. As there is a little information on the leaf structure parameter N considering monocotyledon and dicotyledon plants discrimination [11,15–21], this point may also deserve to be investigated in detail for copper-stressed vegetation in the future.

The simulated spectra from PROSPECT-5 are obviously higher than the measured spectra for copper-stressed leaves, while the simulated results from the new model are much nearer to the measured results (Figures 7 and 8). As previously mentioned, the copper content in normal leaf is relatively low (5 mg/kg to 30 mg/kg), but it is able to exceed 1300 mg/kg in a copper-stressed leaf. For normal leaves, the absorption by copper could be ignored and satisfying results could be acquired by PROSPECT-5. For copper-stressed leaves, excessive copper should be considered, and thus better results were acquired by the new model (Figures 7 and 8; Tables 3 and 4). Specifically, PROSPECT-5 was designed for healthy leaves, so it ignores the energy absorbed by copper-related matter, which leads to higher simulated reflectance for copper-stressed leaves. This is the reason why the simulated spectra from the modified model are much nearer to the measurements and the RMSEs with the modified model are less.

For the specific absorption coefficient related to copper (K_{cu}), Figure 6 suggests that it almost equals zero in the wavelength range of 400–510 nm, which is different from the results in [23]. However, the absorption spectra of aqueous copper sulfate solutions measured strictly in the laboratory [24], is consistent with the results in our study at 400–510 nm, which indicates that our results are more reasonable than that in [23].

The high values of K_{cu} at 590–710 nm, near 1400 nm, 1900 nm and 2400 nm, agree with the results in [23,30] well. For the explanation on the apparent characteristics near 1400 nm and 1900 nm, Zhu et al. [23] simply pointed that the coordinate bonds with hydroxide contribute to the observed features near 1400 nm and 1900 nm. Here, we try to give a more detailed explanation on all the observed features at 590–710 nm, 1400 nm, 1900 nm and 2400 nm. For copper-stressed vegetation, excessive copper in the soil was easily absorbed by plants via Cu^{2+} and $Cu(OH)^+$. In leaves, the Cu^{2+} and $Cu(OH)^+$ were transferred into chelate and fixed in organelle to hinder copper from diffusing and to protect other tissues in the plant [30,31]. According to the spectral theory, reflectance at 400–1300 nm is controlled by the electron transition of metal ions, while reflectance at 1300–2500 nm is determined by anionic group (e.g., hydroxyl, carbonate, sulfate) [32,33]. In this study, the high values of K_{cu} at 590–710 nm are similar with the absorption of copper sulfate and copper chloride [23,30], and the high values near 1400 nm and 1900 nm are similar with the absorption of water [22]. Hence, it can be inferred that Cu^{2+} contributes to the absorption at 590–710 nm, and hydroxyl contributes to the absorption near 1400 nm and 1900 nm. Sulfate ion shows absorption at 2400 nm [34]. The vegetation in this study was treated by copper sulfate ($CuSO_4$), so it was inferred that sulfate ions contributed to the high values of K_{cu} near 2400 nm. In addition, it appeared that the valley near 680 nm of K_{cu} could be observed. Vegetation stress always induces the enhancement of chlorophyll fluorescence [35–37]. According to the shape of chlorophyll fluorescence [35,38], it can be inferred that a high chlorophyll

fluorescence (red fluorescence, RF) is also present near 680 nm. Thus, idealized K_{cu} needed to be reduced to enlarge the simulated reflectance to meet the enhancement from chlorophyll fluorescence. Therefore, RF is a very possible factor that makes contributions to this valley. Chlorophyll fluorescence also possesses high values called blue green fluorescence (BGF), ranging from approximately 350 nm to 520 nm [35,38], so some measured spectra are higher than simulated spectra generated by both PROSPECT-5 and the modified model in the visible range (Figure 7). In other words, this problem was also present in PROSPECT-5. K_{cu} is near zero in this wavelength range (Figure 6), so the enhancement on measured reflectance from BGF cannot be meted by reducing K_{cu}. Hence, chlorophyll fluorescence should be removed from the measured reflectance in the future to improve the ability to predict the spectra in the visible range. In total, K_{cu} reflects the overall influence from copper ion and its chelate, and other factors induced by copper, so we tentatively termed K_{cu} "specific absorption coefficient related to copper", not "specific absorption coefficient of copper ion". Moreover, copper stress impacts the leaf structure parameter N and we also changed the wavelength range for estimating N due to the copper presence. Hence, the modified model considers the physiological reaction of the leaf to copper presence, not just adding copper to the leaf spectra. In the future, what biochemical components that make contribution to the specific absorption coefficient related to copper (K_{cu}) and the mechanism of these absorptions should be further investigated and clarified. In addition, based the work in this paper, estimating the copper content in leaves and classifying the vegetation with different copper contamination using remote sensing could also be the basis of a good future study.

In terms of other advantages, this study would help the research on remote sensing of stressed vegetation. For example, similar changes in reflectance and vegetation indices may be resulted from copper stress as well as other stress [39–41], but this study provided some physical foundations to distinguish copper stress from other stress.

In this study, the soil before treatments was collected from vegetable garden without any contamination. In general, the copper content in this kind of soil is <2 mg/kg [42,43]. The increments of copper content in the soil after treatments are 25, 50, 100, . . . , 4800 mg/kg. Hence, the copper content in the soil at a minimum stress level exceeds that in the normal soil by 10 times. The initial copper content in soil almost has no impact. In fact, the use of the numbers, including 25, 50, 100, . . . , 4800, are simply labels to distinguish the different stress levels. In general, the vegetation can be regarded as copper-stressed vegetation if the growth and biochemical components are obviously influenced when excessive copper is present in the soil, water and the atmosphere [4,44,45]. Kabata-Pendias et al. [44] indicated that vegetation activities would be stressed when the copper content in soil amounted to two to 10 times that in normal soil. Hence, the vegetation could be called copper-stressed vegetation in this paper.

Compared with normal leaves, copper-stressed leaves have been verified that the leaf structure is disrupted and copper content significantly increases [4,45]. The data in this study also illustrates these facts to some degree. Moreover, the simulated reflectance generated by the measured contents of biochemical components (the measurements are regarded as correct) and the standard PROSPECT-5 model was away from the measured reflectance. Based on above facts, we set two hypothesis: (1) the disruption of leaf structure resulted in the increase of N; (2) the increase of copper content resulted in more absorption of energy. Thus, the modification strategy is estimating N in the wavelength range where copper absorption is near to zero, and estimating the specific absorption coefficient related to copper using correct N. This modification strategy is regarded as reasonable. In this sense, this approach also has some physical basis. In the future, others may propose more reasonable approaches to get similar output reflectance. However, the mentioned two hypothesis have not been absolutely verified since Figure 5c is not a good proof and it shows that the approach is not statistically robust. K_{cu} reflects the overall effects from copper stress, not only the absorption of copper ions. Moreover, the tolerance to copper stress varies with different vegetation. From this point of view, the approach in this study is empirical, and not a true physical modification approach. As previously mentioned, other modification approaches may provide the same total output reflectance with that in this study.

For example, if the contents of biochemical components were measured incorrectly, the obtained results in this study, in terms of the accuracy, may be obtained using standard PROSPECT-5 model by changing the *N* value and the effective content of water in the leaf, and maybe of pigments as well.

There is a difference between this study and the studies on remote sensing of normal vegetation. The samples with copper-stressed vegetation are much more difficult to acquire due to experimental complexity. Therefore, the number of samples in many studies related to copper-stressed vegetation is similar to this study (e.g., [46,47]). Even so, we have also realized that more datasets should be used to improve the specific absorption coefficient related to copper (K_{cu}) to further advance the new model. Both the modified model and PROSPECT-5 are based on the leaf scale. LAI (Leaf Area Index) and view and illumination geometry are usually in canopy models, which were not considered in this study. The application of the modified model on remote sensing image needs the coupling with reflectance models at the canopy scale, for example, the SAIL model. The coupling with canopy reflectance model could provide an effective and rapid way for monitoring copper-stressed vegetation on a large scale using remote sensing image, which is also the basis for good future work.

6. Conclusions

This study developed a new model for copper-stress leaves based on PROSPECT-5, and validations were conducted. In this study, the reflectance at 400–510 nm was used to estimate leaf structure parameters (*N*) of copper-stress leaves. The absorption related to copper was considered, and the specific absorption coefficient related to copper (K_{cu}) was estimated. The new model includes six inputs: leaf structure parameters (*N*); chlorophyll content; carotenoid content; equivalent water thickness; dry matter content, and; copper content. Factors that influence the reflectance of copper-stressed leaves are considered as much as possible. The new model shows better performance than PROSPECT-5 on copper-stressed leaves. Hence, this study solved some problems left by previous studies and developed a better model for simulating the copper-stressed leaves, and provides theoretical support for the research on copper-stressed vegetation using remote sensing. Moreover, it has potential significance for prospecting copper deposit and monitoring environmental pollution caused by copper. However, due to the difficulties on the acquirement of datasets of copper-stressed vegetation, more samples should be acquired and used to improve the specific absorption coefficient related to copper (K_{cu}) and the accuracy of new model in the future.

Author Contributions: Chengye Zhang and Huazhong Ren proposed the idea and processed the data, and also participated in the writing of the paper; Yanzhen Liang analyzed the data and the results; Suhong Liu participated in the collection of the data and processed the data; Qiming Qin also analyzed the data and the results; Okan K. Ersoy contributed to the writing of the paper.

Conflicts of Interest: The authors declare no conflict of interest.

References

1. Lulla, K. Some observations on geobotanical remote sensing and mineral prospecting. *Can. J. Remote Sens.* **1985**, *11*, 17–38. [CrossRef]
2. Labovitz, M.L.; Masuoka, E.J. The influence of auto-correlation in signature extraction—An example from a geobotanical investigation of Cotter Basin, Montana. *Int. J. Remote Sens.* **1984**, *5*, 315–332. [CrossRef]
3. Hede, A.N.H.; Koike, K.; Kashiwaya, K.; Sakurai, S.; Yamada, R.; Singer, D.A. How can satellite imagery be used for mineral exploration in thick vegetation areas? *Geochem. Geophys. Geosyst.* **2017**, *18*, 584–596. [CrossRef]

4. Wang, J.; Wang, T.; Shi, T.; Wu, G.; Skidmore, A.K. A Wavelet-based area parameter for indirectly estimating copper concentration in carex leaves from canopy reflectance. *Remote Sens.* **2015**, *7*, 15340–15360. [CrossRef]

5. Kong, W.; Huang, W.; Zhou, X.; Song, X.; Casa, R. Estimation of carotenoid content at the canopy scale using the carotenoid triangle ratio index from in situ and simulated hyperspectral data. *J. Appl. Remote Sens.* **2016**, *10*. [CrossRef]

6. Liu, S.; Liu, X.; Hou, J.; Chi, G.; Cui, B. Study on the spectral response of *Brassica Campestris* L. leaf to the copper pollution. *Sci. China Technol. Sci.* **2008**, *51*, 202–208. [CrossRef]

7. Emengini, E.J.; Blackburn, G.A.; Theobald, J.C. Discrimination of plant stress caused by oil pollution and waterlogging using hyperspectral and thermal remote sensing. *J. Appl. Remote Sens.* **2013**, *7*. [CrossRef]

8. Gitelson, A.A.; Gritz, Y.; Merzlyak, M.N. Relationships between leaf chlorophyll content and spectral reflectance and algorithms for non-destructive chlorophyll assessment in higher plant leaves. *J. Plant Physiol.* **2003**, *160*, 271–282. [CrossRef] [PubMed]

9. Herrmann, I.; Berenstein, M.; Paz-Kagan, T.; Sade, A.; Karnieli, A. Spectral assessment of two-spotted spider mite damage levels in the leaves of greenhouse-grown pepper and bean. *Biosyst. Eng.* **2017**, *157*, 72–85. [CrossRef]

10. Sanchez, R.A.; Hall, A.J.; Trapani, N.; Dehunau, R.C. Effects of water-stress on the chlorophyll content, nitrogen level and photosynthesis of leaves of 2 maize genotypes. *Photosynth. Res.* **1983**, *4*, 35–47. [CrossRef] [PubMed]

11. Jacquemoud, S.; Baret, F. PROSPECT—A model of leaf optical-properties spectra. *Remote Sens. Environ.* **1990**, *34*, 75–91. [CrossRef]

12. Jacquemoud, S.; Verhoef, W.; Baret, F.; Bacour, C.; Zarco-Tejada, P.J.; Asner, G.P.; Francois, C.; Ustin, S.L. PROSPECT plus SAIL models: A review of use for vegetation characterization. *Remote Sens. Environ.* **2009**, *113*, S56–S66. [CrossRef]

13. Allen, W.A.; Gausman, H.W.; Richardson, A.J.; Thomas, J.R. Interaction of isotropic light with a compact plant leaf. *J. Opt. Soc. Am.* **1969**, *59*, 1376–1379. [CrossRef]

14. Allen, W.A.; Gausman, H.W.; Richardson, A.J. Mean effective optical constants of cotton leaves. *J. Opt. Soc. Am.* **1970**, *60*, 542–547. [CrossRef]

15. Fourty, T.; Baret, F.; Jacquemoud, S.; Schmuck, G.; Verdebout, J. Leaf optical properties with explicit description of its biochemical composition: Direct and inverse problems. *Remote Sens. Environ.* **1996**, *56*, 104–117. [CrossRef]

16. Jacquemoud, S.; Ustin, S.L.; Verdebout, J.; Schmuck, G.; Andreoli, G.; Hosgood, B. Estimating leaf biochemistry using the PROSPECT leaf optical properties model. *Remote Sens. Environ.* **1996**, *56*, 194–202. [CrossRef]

17. Baret, F.; Fourty, T. Estimation of leaf water content and specific leaf weight from reflectance and transmittance measurements. *Agronomie* **1997**, *17*, 455–464. [CrossRef]

18. Fourty, T.; Baret, F. On spectral estimates of fresh leaf biochemistry. *Int. J. Remote Sens.* **1998**, *19*, 1283–1297. [CrossRef]

19. Jacquemoud, S.; Bacour, C.; Poilve, H.; Frangi, J.P. Comparison of four radiative transfer models to simulate plant canopies reflectance: Direct and inverse mode. *Remote Sens. Environ.* **2000**, *74*, 471–481. [CrossRef]

20. Le Maire, G.; Francois, C.; Dufrene, E. Towards universal broad leaf chlorophyll indices using PROSPECT simulated database and hyperspectral reflectance measurements. *Remote Sens. Environ.* **2004**, *89*, 1–28. [CrossRef]

21. Feret, J.; Francois, C.; Asner, G.P.; Gitelson, A.A.; Martin, R.E.; Bidel, L.P.R.; Ustin, S.L.; le Maire, G.; Jacquemoud, S. PROSPECT-4 and 5: Advances in the leaf optical properties model separating photosynthetic pigments. *Remote Sens. Environ.* **2008**, *112*, 3030–3043. [CrossRef]

22. Bousquet, L.; Lacherade, S.; Jacquemoud, S.; Moya, I. Leaf BRDF measurements and model for specular and diffuse components differentiation. *Remote Sens. Environ.* **2005**, *98*, 201–211. [CrossRef]

23. Zhu, Y.; Qu, Y.; Liu, S.; Chen, S. A reflectance spectra model for copper-stressed leaves: Advances in the PROSPECT model through addition of the specific absorption coefficients of the copper ion. *Int. J. Remote Sens.* **2014**, *35*, 1356–1373. [CrossRef]

24. Jancso, G. Effect of D and O-18 isotope substitution on the absorption spectra of aqueous copper sulfate solutions. *Radiat. Phys. Chem.* **2005**, *74*, 168–171. [CrossRef]

25. Kubalova, I.; Ikeda, Y. Chlorophyll measurement as a quantitative method for the assessment of cytokinin-induced green foci formation in tissue culture. *J. Plant Growth Regul.* **2017**, *36*, 516–521. [CrossRef]

26. Arevalo-Gardini, E.; Arevalo-Hernandez, C.O.; Baligar, V.C.; He, Z.L. Heavy metal accumulation in leaves and beans of cacao (*Theobroma cacao* L.) in major cacao growing regions in Peru. *Sci. Total Environ.* **2017**, *605*, 792–800. [CrossRef] [PubMed]

27. Hosgood, B.; Jacquemoud, S.; Andreoli, G.; Verdebout, J.; Pedrini, G.; Schmuck, G. *Leaf Optical Properties Experiment 93 (LOPEX93)*; European Commission: Brussels, Belgium, 1994.

28. OPTICALEAF-Database. Available online: http://opticleaf.ipgp.fr/index.php?page=database (accessed on 10 February 2017).

29. Li, X.; Liu, X.; Liu, M.; Wang, C.; Xia, X. A hyperspectral index sensitive to subtle changes in the canopy chlorophyll content under arsenic stress. *Int. J. Appl. Earth Obs.* **2015**, *36*, 41–53. [CrossRef]

30. Zhou, C. Research on Retrieval Method of Heavy Metal Content of Vegetation Using Hyperspectral Remote Sensing. Ph.D. Thesis, Jilin University, Changchun, China, 2016.

31. Wu, W. *Plant Physiology*, 2nd ed.; Science Press: Beijing, China, 2008; ISBN 9787030224132.

32. Van der Meer, F.D.; van der Werff, H.M.A.; van Ruitenbeek, F.J.A.; Hecker, C.A.; Bakker, W.H.; Noomen, M.F.; van der Meijde, M.; Carranza, E.J.M.; de Smeth, J.B.; Woldai, T. Multi- and hyperspectral geologic remote sensing: A review. *Int. J. Appl. Earth Obs.* **2012**, *14*, 112–128. [CrossRef]

33. Zhang, C.; Qin, Q.; Chen, L.; Wang, N.; Zhao, S.; Hui, J. Rapid determination of coalbed methane exploration target region utilizing hyperspectral remote sensing. *Int. J. Coal Geol.* **2015**, *150*, 19–34. [CrossRef]

34. Bishop, J.L.; Parente, M.; Catling, D. Juventae Chasma as Potential MSL Landing Site. In Proceeding of the 2nd MSL Landing Site Workshop, Old Town Pasadena, CA, USA, 23–25 October 2007; Available online: https://marsoweb.nas.nasa.gov/landingsites/msl/workshops/2nd_workshop/talks/Bishop_Juventae.pdf (accessed on 13 November 2017).

35. Qu, Y.; Liu, S.; Li, X. A novel method for extracting leaf-level solar-induced fluorescence of typical crops under Cu stress. *Spectrosc. Spectr. Anal.* **2012**, *32*, 1282–1286.

36. Chou, S.; Chen, J.M.; Yu, H.; Chen, B.; Zhang, X.; Croft, H.; Khalid, S.; Li, M.; Shi, Q. Canopy-level photochemical reflectance index from hyperspectral remote sensing and leaf-level non-photochemical quenching as early indicators of water stress in maize. *Remote Sens.* **2017**, *9*, 794. [CrossRef]

37. Rascher, U.; Alonso, L.; Burkart, A.; Cilia, C.; Cogliati, S.; Colombo, R.; Damm, A.; Drusch, M.; Guanter, L.; Hanus, J.; et al. Sun-induced fluorescence—A new probe of photosynthesis: First maps from the imaging spectrometer HyPlant. *Glob. Chang. Biol.* **2015**, *21*, 4673–4684. [CrossRef] [PubMed]

38. Zarco-Tejada, P.J.; Miller, J.R.; Mohammed, G.H.; Noland, T.L. Chlorophyll fluorescence effects on vegetation apparent reflectance: I. Leaf-level measurements and model simulation. *Remote Sens. Environ.* **2000**, *74*, 582–595. [CrossRef]

39. Ghulam, A.; Fishman, J.; Maimaitiyiming, M.; Wilkins, J.L.; Maimaitijiang, M.; Welsh, J.; Bira, B.; Grzovic, M. Characterizing crop responses to background ozone in open-air agricultural field by using reflectance spectroscopy. *IEEE Geosci. Remote Sens.* **2015**, *12*, 1307–1311. [CrossRef]

40. Zhang, C.; Ren, H.; Qin, Q.; Ersoy, O.K. A new narrow band vegetation index for characterizing the degree of vegetation stress due to copper: The copper stress vegetation index (CSVI). *Remote Sens. Lett.* **2017**, *8*, 576–585. [CrossRef]

41. Yang, X.; Chen, L. Evaluation of automated urban surface water extraction from Sentinel-2A imagery using different water indices. *J. Appl. Remote Sens.* **2017**, *11*. [CrossRef]

42. Fan, Y.; Lu, Y.; Li, F.; Xue, J.; Li, X.; Zhong, B.; Peng, L. Study on distribution of available copper content in soil of navel orange orchards in southern Jiangxi Province. *J. Fruit Sci.* **2015**, *32*, 69–73. [CrossRef]

43. Li, Z.; Yi, W. Present status and improvement countermeasures of the soil fertility of vegetable fields in Guangzhou suburb. *Guangdong Agric. Sci.* **2008**, *2*, 43–46. [CrossRef]

44. Kabata-Pendias, A.; Pendias, H. *Trace Element in Soil and Plants*; CRC Press: Boca Raton, FL, USA, 1984.

45. Hall, J. Cellular mechanisms for heavy metal detoxification and tolerance. *J. Exp. Bot.* **2002**, *53*, 1–11. [CrossRef] [PubMed]

46. Asmaryan, S.; Warner, T.A.; Muradyan, V.; Nersisyan, G. Mapping tree stress associated with urban pollution using the WorldView-2 Red Edge band. *Remote Sens. Lett.* **2013**, *4*, 200–209. [CrossRef]

47. Rathod, P.H.; Brackhage, C.; van der Meer, F.D.; Mueller, I.; Noomen, M.F.; Rossiter, D.G.; Dudel, G.E. Spectral changes in the leaves of barley plant due to phytoremediation of metals—Results from a pot study. *Eur. J. Remote Sens.* **2005**, *48*, 283–302. [CrossRef]